Cellular Physiology and Biochemistry

Cell Physiol Biochem 2018;51:1500-1517
DOI: 10.1159/000495641
Published online: 29 November 2018
Accepted: 21 November 2018

Original Paper

Characterization of the Nucleocytoplasmic Transport Mechanisms of Epstein-Barr Virus BFLF2

Meili Li[a,b] Tao Chen[b] Xingmei Zou[b] Zuo Xu[b] Yuanfang Wang[b] Ping Wang[b] Xiaowen Ou[b] Yiwen Li[b] Daixiong Chen[b] Tao Peng[c,d] Yao Wang[e] Mingsheng Cai[b]

[a]Guangdong Provincial Key Laboratory of Allergy and Clinical Immunology, Second Affiliated Hospital of Guangzhou Medical University, Guangzhou, [b]Department of Pathogenic Biology and Immunology, Sino-French Hoffmann Institute, School of Basic Medical Science, Guangzhou Medical University, Xinzao Town, [c]State Key Laboratory of Respiratory Diseases, Sino-French Hoffmann Institute, School of Basic Medical Science, Guangzhou Medical University, Xinzao Town, [d]South China Vaccine Corporation Limited, Guangzhou Science Park, Guangzhou, [e]GMU-GIBH Joint School of Life Sciences, Guangzhou Medical University, Xinzao Town, China

Key Words
BFLF2 • Nuclear transport • Nuclear localization signal (NLS) • Nuclear export signal (NES) • Importin • Ran-GTP

Abstract
Background/Aims: Epstein-Barr virus (EBV) BFLF2, the homologue of herpes simplex virus 1 (HSV-1) UL31, is crucial for the efficient viral DNA packaging and primary egress across the nuclear membrane. However, we still do not know its subcellular transport mechanisms. ***Methods:*** Interspecies heterokaryon assays were utilized to detect the nucleocytoplasmic shuttling of BFLF2, and mutation analysis, plasmid transfection and fluorescence microscopy assays were performed to identify the functional nuclear localization sequence (NLS) and nuclear export sequence (NES) of BFLF2 in live cells. Furthermore, the nuclear import and export of BFLF2 were assessed by confocal microscopy, co-immunoprecipitation and immunoblot assays. ***Results:*** BFLF2 was confirmed to shuttle between the nucleus and cytoplasm. Two predicted NESs were shown to be nonfunctional, yet we proved that the nuclear export of BFLF2 was mediated through transporter associated with antigen processing (TAP), but not chromosomal region maintenance 1 (CRM1) dependent pathway. Furthermore, one functional NLS, ^{22}RRLMHPHHRNYTASKASAH^{40}, was identified, and the aa22-23, aa22-25, aa28-30 and aa37-40 had an important role in the nuclear localization of BFLF2. Besides, the nuclear import of BFLF2 was demonstrated through Ran-, importin α7-, importin β1- and transportin-1-dependent mechanism that does not require importin α1, α3 and α5. ***Conclusion:*** These works

M. Li and T. Chen contributed equally to this work.

Mingsheng Cai Guangdong Provincial Key Laboratory of Allergy and Clinical Immunology, Second Affiliated Hospital of Guangzhou Medical University, No.250 Changgang Dong Road, Haizhu District, Guangzhou 510260, Guangdong (China), Tel. (96) 020-37103216, E-Mail mingshengcai@hotmail.com

are of significance for the further study of the functions of BFLF2 during EBV infection, as well as for further insights into the design of new antiviral drug target and vaccine development against EBV.

Introduction

Epstein-Barr virus (EBV), also known as human herpesvirus 4, is a gammaherpesvirus that infects the majority of the world's population [1]. EBV is also associated with the development of certain malignancies, including African Burkitt lymphomas, B-cell lymphomas of immunocompromised patients, nasopharyngeal carcinomas, Hodgkin's disease, and occasionally with T-cell lymphomas and gastric cancers [2]. The EBV genome is composed of linear double-stranded DNA, with approximately 172 kilobase pairs in length [3], which encodes about 86 proteins [4]. According to their localization in the virions, the proteins could be divided into five groups: envelope, tegument, capsid, and unclassified and nonstructural proteins. This complicated network of proteins leads to various consequences on the host cell and guarantees efficient viral proliferation [3].

Viruses possess many strategies to impair host cellular responses to infection, and virus replicates in the nucleus must compete with host mRNAs to efficiently export their viral mRNAs to express proteins that are necessary for further replication and/or nascent virion assembly. EBV is a well known DNA virus to interact with different nuclear export factors and co-opt many cellular proteins for replication within the nucleus, and transport of viral transcripts to the cytoplasm for protein synthesis [5].

Active transport of protein between the nucleus and cytoplasm depends on the presence of nuclear localization signal (NLS) and nuclear export signal (NES) [6]. Two nuclear export receptors have been shown to be responsible for the export of protein and mRNA. The first identified chromosomal region maintenance 1 (CRM1, also known as XPO1 and exportin 1) recognizes NES that consists of short hydrophobic stretches [7]. Another receptor is the human transporter associated with antigen processing (TAP, also called nuclear export factor 1 (NXF1), which is the best candidate for mRNA export, since it has been shown to shuttle between the nucleus and cytoplasm, and cross-link to poly(A)$^+$ RNA [8]. Besides, the importin α/β complex and GTPase Ran can mediate the nuclear import of proteins with a classical NLS [9], which composes of basic amino acid (aa) residues [6]. Like other GTPases, Ran requires effectors to help it hydrolyze GTP and exchange the formed guanosine diphosphate (GDP) for GTP [8-10].

Most of the viral structures contain a capsid, and a majority of the virions identified outside the nucleus also carry viral DNA with the help of some viral proteins, such as EBV BFLF2, the homologue of herpes simplex virus 1 (HSV-1) UL31, varicella-zoster virus (VZV) ORF27, murine cytomegalovirus (MCMV) M53 and Kaposi's sarcoma-associated herpesvirus (KSHV) ORF69 [11]. During HSV-1 infection, UL31 forms a complex with UL34 at the cellular nuclear membrane, where both proteins play important roles in the envelopment of viral nucleocapsids and their egress into the cytoplasm [12]. Moreover, VZV ORF27/ORF24, MCMV M53/M50 and KSHV ORF69/ORF67 also have been confirmed to comprise a nuclear egress complex at the nuclear membrane in the export of nascent virus capsids [11, 13-15].

It's shown that BFLF2 and BFRF1 compose the nuclear lamina and take a critical role in the early step of EBV maturation at the nuclear membrane [16, 17]. Previous study reported that deletion of BFLF2 can impair the viral DNA packaging and primary egress of EBV, as well as the increase production of defective viral particles [18]. BFLF2 is a nuclear phosphoprotein of approximately 35 kDa, expressed early during viral replicative cycle, but is not detectable in extracellular virions [16]. Our recent study showed that BFLF2 localizes absolutely to the nucleus [3], which is in accordance with the subcellular localization of HSV-1 UL31 [19, 20]. However, the determining mechanisms for its subcellular transport

were not well understood, thus prompting us to investigate the nucleocytoplasmic transport mechanisms of BFLF2.

In the present study, BFLF2 was demonstrated to shuttle between the nucleus and the cytoplasm through TAP/NXF1, RanGTP, importin α7, importin β1 and transportin-1 dependent pathway.

Materials and Methods

Cells, antibodies and reagents

COS-7 cells, NIH3T3 cells and HEK293T cells were cultured in Dulbecco's modified MEM (DMEM, Gibco-BRL) supplemented with 10% fetal bovine serum (FBS; Gibco-BRL) in a humidified atmosphere containing 5% CO2 at 37 °C. HONE1-EBV cells (gift from Prof. S.W. Tsao, University of Hong Kong) are EBV positive nasopharyngeal carcinoma cell lines [21], which were cultured in RPMI-1640 (Gibco-BRL) medium supplemented with 10% FBS. Mouse monoclonal antibody (mAb) anti-Flag was purchased from Abmart (Shanghai, China) and rabbit polyclonal antibody (pAb) anti-YFP was purchased from RayBiotech. Mouse nonspecific IgG was offered by eBioscience (China), mouse anti-BFLF2 pAb was prepared in our lab by inoculating mouse with the purified BFLF2 protein expressed in *E. coli* BL21. The protein A/G Plus-agarose was purchased from Santa Cruz.

Plasmid construction

All enzymes used for cloning were purchased from Thermo Scientific except DNA polymerase KOD-Plus-Neo from TOYOBO and T4 DNA Ligase from Takara. The BFLF2 open reading frame (ORF) was polymerase chain reaction amplified from BAC DNA of EBV B95-8 strain (174-kb BAC) [3, 22], then the product was digested with *E*coRI and *B*amHI and inserted into the green fluorescent protein variant mammalian expression vector pEYFP-N1 (Clontech, BD Biosciences, Palo Alto, CA) encoding enhanced yellow fluorescent protein (EYFP), to creat pBFLF2-EYFP. Fragments and mutants of BFLF2 were inserted into pEYFP-C1 (Clontech, BD Biosciences) to analyze the functions of the predicted NLS and NES. pEYFP-BFLF2, pEYFP-BKRF2 and pFLAG-CMV-transportin-1 were constructed in our lab previously [3, 23].

Other plasmids listed below were also constructed, as described above. BFRF1 was cloned into pmCherry-N1 (Clontech, BD Biosciences) and pCMV-Flag-N1 (Beyotime Biotechnology), to creat pBFRF1-mCherry and pBFRF1-Flag, respectively. BZLF1 was cloned into pHA-N1 vector (Clontech) to creat pBZLF1-HA-N1. HSV-1 (F strain) UL6 from pYEbac102 [24] was cloned into pEYFP-C1 to generate pEYFP-UL6. pBFLF2(NLS)-EYFP-BKRF2 was yielded by inserting the oligonucleotides of BFLF2 NLS into the *B*glII and *H*indⅢ digested pEYFP-BKRF2. TAP, dominant negative (DN) mutant RanGTP (Ran-Q69L) [25], DN kα1 (importin α5) [26] and DN kβ1 (importin β1) [27] were subcloned into pmCherry-N1 to yield pTAP-mCherry, pRan-Q69L-mCherry, pDN kα1-mCherry and pDN kβ1-mCherry, respectively. All constructs were confirmed by DNA sequencing, and primers used in this study are available upon request.

Besides, plasmid pnucleolin-EGFP was a generous gift from Dr. Johannes A. Schmid [28] and used as a nucleolar marker. M9M-RFP and Bimax2-RFP were generous gifts from Dr. Nobuyuki Nukina [29]. Moreover, plasmids expressing Flag-kα1 (importin α5), Flag-kα6 (importin α7) [30], Flag-kα2 (importin α1), Flag-kα4 (importin α3) [31] and pCMV9-3×Flag-importinβ1 were generously supplied by Drs. Yoshihiro Yoneda, Reinhard Depping and Ben Margolis, respectively. pFLAG-CMV-TAP was generous gifts from Dr. Chunfu Zheng [32]. Plasmid pEYFP-UL54 (derived from pseudorabies virus, (PRV)), which used as a control for the TAP-dependent pathway, was described previously [32].

Transfection and fluorescence microscopy

To test the subcellular localizations of various proteins in live cells, plasmid transfection and fluorescence microscopy assays were performed as described in our previous studies [3, 19, 23, 33, 34]. Briefly, COS-7 cells were placed onto 12 well plates (Corning, USA) in DMEM with 10% FBS overnight to reach the confluency 70-80% before transfection. The next day, monolayer cells were transfected with 1-1.5μg of the indicated plasmid DNA mixed with polyetherimide, as per the manufacturer's instructions. After transfection for 24 h, the live cells were analyzed using fluorescence microscopy.

Interspecies heterokaryon assay

Nucleocytoplasmic shuttling was detected using an interspecies heterokaryon assay, as described with modification [35, 36]. Co-culture of transfected COS-7 and NIH3T3 cells were allowed to grow for 4 h at 37°C. Protein synthesis was blocked with 50 μg/mL cycloheximide 30 min prior to the fusion and throughout the experiment. If inhibition of CRM1-dependent protein export was required, cells were treated additionally with 20 ng/mL leptomycin B (LMB) (Sigma) 3 h before cell fusion. Subsequently, cells were washed with PBS, and heterokaryons were formed by incubating the cells for 2 min in 50% polyethylene glycol (PEG) 1300-1600 in Hanks' balanced media (Gibco). Following cell fusion, cells were washed extensively in PBS and returned to fresh medium containing 50 μg/mL cycloheximide and 5 ng/mL LMB when needed. After 1 h, cells were detected by fluorescence microscopy for EYFP fusion protein with 4',6'-diamidino-2-phenylindole (DAPI) (Vector Laboratories) staining when needed. At least 50 karyons were analyzed for each experiment and nuclear shuttling was only scored positive when a minimum of 80% of the heterokaryons showed a positive staining of the investigated protein.

Confocal microscopy

COS-7 cells plated on glass coverslips in six-well plates (Corning, USA) were co-transfected with the indicated plasmids for 24 h, and fixed with 4% paraformaldehyde for 30 min, then stained with DAPI for 5 min, and examined by laser scanning confocal microscopy (Leica SP8).

RNA isolation

HEK293T cells were collected and quickly frozen on dry ice. Total RNA was extracted using Trizol (Invitrogen, CA, USA) according to the manufacturer's manual. Samples were then digested with DNase I to remove trace amounts of contaminating DNA. The integrity of the total RNA was monitored by running a 1.2% agarose gel with 0.5 to 1 μg of extracted RNA [32, 37].

Co-immunoprecipitation and immunoblot

Co-immunoprecipitation (Co-IP) and immunoblot (IB) were performed as described previously [19, 20, 23, 34, 38, 39]. HEK293T cells were co-transfected with 10 μg of each of the indicated expression plasmids carrying FLAG or EYFP tag. Simultaneously, HONE1-EBV cells were firstly transfected with 10 μg of each of the indicated expression plasmids, and then transfected with expression plasmid pBZLF1-HA (10 μg) 12 h later to induce the lytic replication of EBV for 24 h. Transfected cells (HEK293T cells for 30 h and HONE1-EBV cells for 36 h) were lysed using 700 μl cell lysis buffer (Beyotime, China) on ice, followed by incubation overnight with the appropriate antibodies plus Protein A/G beads. Beads were washed five times and eluted. All Co-IP assays were repeated at least twice times, and similar data were obtained.

Results

Nucleocytoplasmic shuttling of the BFLF2 protein

If a protein could be exported out of the nuclei of transfected cells and re-imported into the nuclei of un-transfected cells, it is considered to be capable of nucleocytoplasmic trafficking [40]. It's shown that BFLF2 localizes predominantly to the nucleus [3], implying that it may shuttle between the nucleus and cytoplasm. In order to determine whether BFLF2 is a nucleocytoplasmic shuttling protein, an interspecific heterokaryon assay [41] was performed. Firstly, to analyze whether the direction of EYFP impacts the distribution of BFLF2 in COS-7 cells, full-length BFLF2 was cloned to the C-terminus and N-terminus of EYFP, respectively (Fig. 1A). Fluorescence microscope showed BFLF2-EYFP and EYFP-BFLF2 had similar nuclear subcellular localization (Fig. 1B), suggesting the direction of EYFP did not affect the localization of BFLF2. Therefore, we used EYFP-BFLF2 for subsequent experiments. Additionally, pEYFP-BFLF2 and the nucleolar marker nucleolin-EGFP were co-transfected into COS-7 cells, and result demonstrated that BFLF2 could not locate in the nucleolus (Fig. 1C).

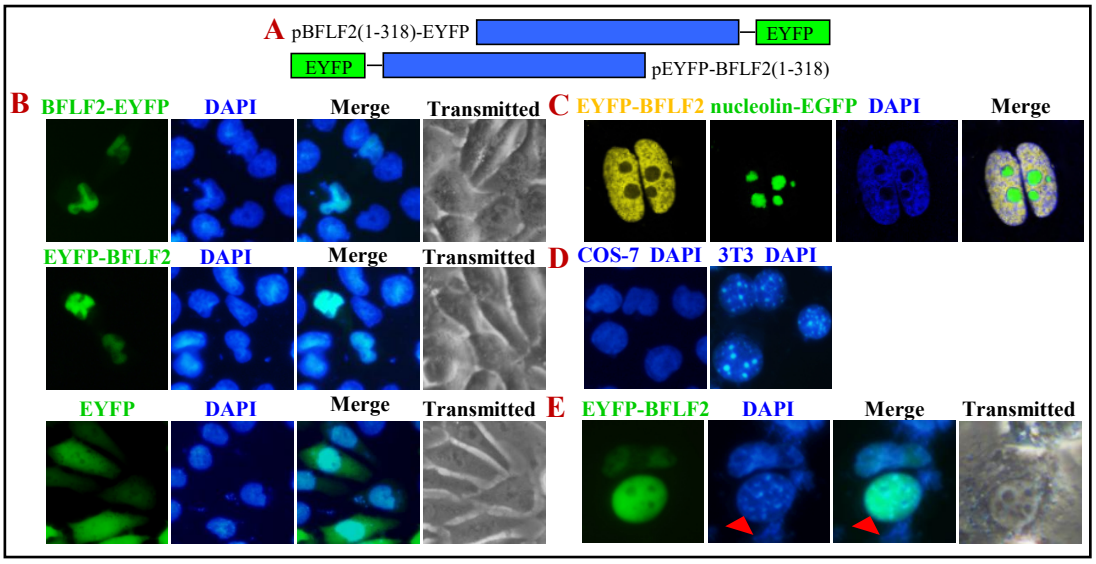

Fig. 1. BFLF2 is a nucleocytoplasmic shuttling protein. (A) Schematic diagram of wild-type BFLF2 fused to the C-terminus and N-terminus of EYFP. (B) Subcellular distribution of full-length BFLF2-EYFP, EYFP-BFLF2 and vector EYFP. (C) COS-7 cells co-transfected with pEYFP-BFLF2 and nucleolin-EGFP expressing plasmids. The nuclei were stained with DAPI (B and C). (D) Differentiation between monkey (COS-7) and mouse (NIH3T3) nuclei by DAPI. (E) COS-7 cells were transfected with EYFP-BFLF2 for 24 h, then transfected cells were subjected to the interspecific heterokaryon assay. DAPI staining and cycloheximide treatment were performed. Mouse NIH3T3 cells were identified by their speckled nuclei when stained with DAPI (the red arrowhead). Each image is representative of the vast majority of the cells observed. Light-translucent pictures show the cellular morphology.

Next, COS-7 cells transfected with EYFP-BFLF2 were fused to an equivalent number of mouse NIH3T3 cells in the presence of protein synthesis inhibitor cycloheximide. To differentiate mouse and monkey nuclei, the cells were stained with DAPI dye. As results, monkey nuclei (COS-7) stained diffusely, whereas mouse nuclei (NIH3T3) exhibited a characteristic speckled pattern (Fig. 1D) [41]. Fusion of NIH3T3 cells to COS-7 cells expressing EYFP-BFLF2 resulted in the presence of EYFP-BFLF2 in the non-expressing mouse NIH3T3 cell nuclei (Fig. 1E), suggesting that BFLF2 could shuttle between the nucleus and the cytoplasm.

Preliminarily characterizating the NLS and NES of BFLF2

Since BFLF2 can shuttle between the cytoplasm and nucleus, there should be particular aa within BFLF2 that are responsible for its shuttling. Bioinformatics analysis showed that BFLF2 does not contain predicted NLS (Fig. 2A), however, the basic aa clusters ^{22}RRLMHPHHR^{30} and ^{71}RHTRH^{75} are possible functional NLSs (Fig. 2B), and the alkaline aa 12, 15, 36 and 40 may be critical for the nuclear localization of BFLF2. Besides, BFLF2 was predicted to possess two leucine-rich NESs, that is NES1 (^{119}LSLCTLSP^{126}) and NES2 (^{291}EAIKDLECGDELRLQII^{307}) (Fig. 2B and 2C). From the above results, we hypothesized that there is a functional NLS in BFLF2, which can guide exogenous protein to the nucleus. Therefore, two deletion mutants encompassing aa1-100 and aa101-381 in frame with EYFP were firstly constructed (Fig. 2D) to investigate their subcellular localizations. As shown in Fig. 2, aa1-100 localized predominantly to the nucleus, while aa101-318 localized evenly throughout the nucleus and cytoplasm (Fig. 2E), these results suggested that aa1-100 contained functional NLS, and aa101-318 might not contain functional NES.

Then, aa1-50, aa51-100, aa101-150 and aa291-318 were constructed to analyze their localizations (Fig. 2D). The fluorescent patterns of aa1-50 was identical to that of aa1-100 and full length BFLF2 (Fig. 2F), while aa51-100, aa101-150 and aa291-318 were distributed

diffusely throughout the cells (Fig. 2F and 2G). These results suggested that the predicted NLS ^{22}RRLMHPHHR^{30}, but not ^{71}RHTRH^{75}, might be functional, and the predicted NES1 (^{119}LSLCTLSP^{126}) and NES2 (^{291}EAIKDLECGDELRLQII^{307}) were not functional. To conclude the functionality of predicted NESs, interspecies heterokaryon assay was performed. As shown in Fig. 2H, COS-7 cells expressing EYFP-BFLF2(aa101-150) or EYFP-BFLF2(aa291-318) fused with mouse NIH3T3 cells could not induce the shuttling of these fusion proteins into the nuclei of NIH3T3 cells, suggesting EYFP-BFLF2(aa101-150) and EYFP-BFLF2(aa291-318) couldn't shuttle between the nucleus and cytoplasm. These results further confirmed that the predicted NES1 and NES2 were not functional.

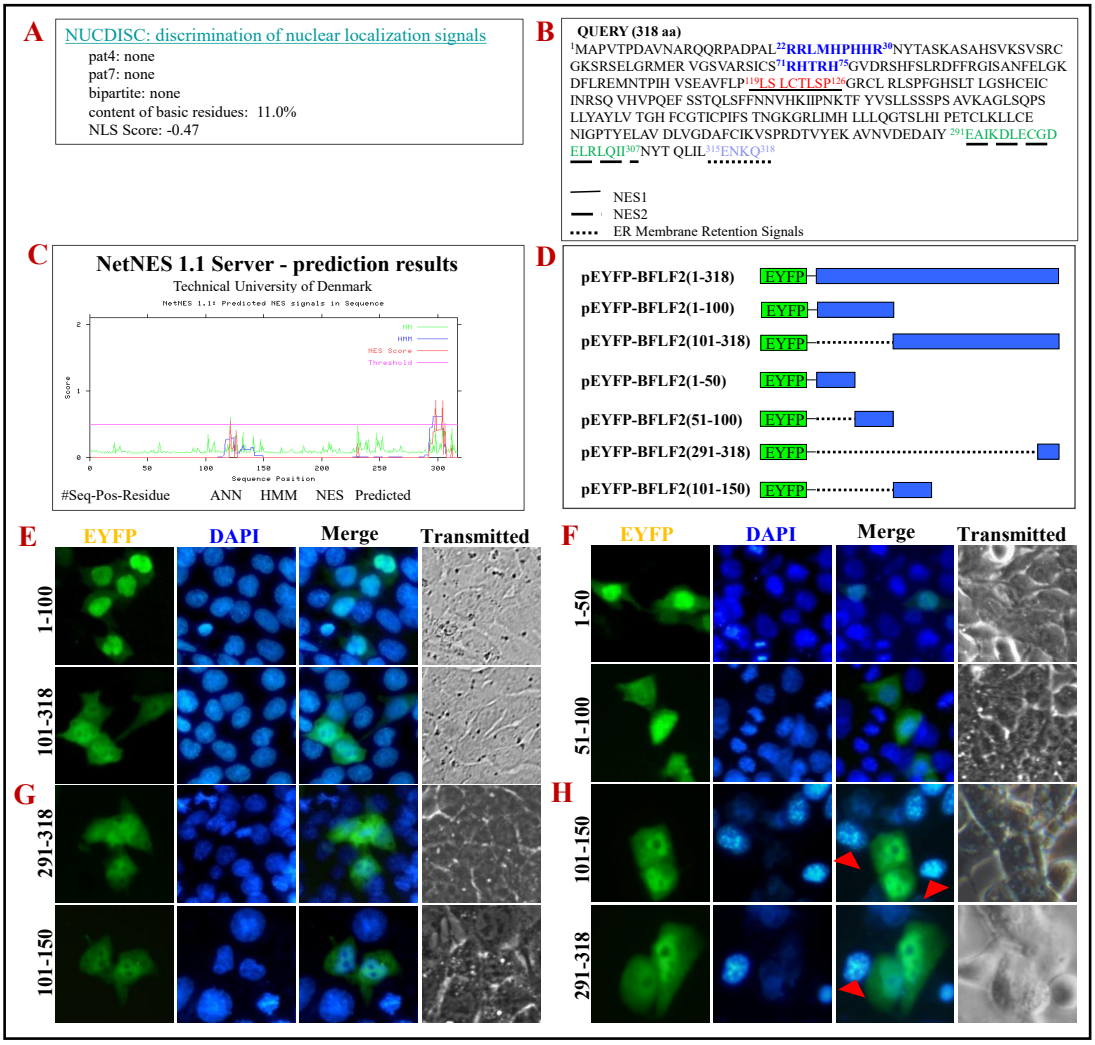

Fig. 2. Preliminarily identifying the NLS and NES of BFLF2. (A) NLS of BFLF2 was predicted with the bioinformatics software PSORT II. (B) Amino acid sequence of the BFLF2 gene. (C) NES of BFLF2 was predicted with the bioinformatics software NetNES 1.1. (D) Schematic representation of BFLF2 protein and its deletion mutants fused to the C-terminus of EYFP. (E) Subcellular localizations of deletion mutants aa1-100 and aa101-318. (F) Subcellular localizations of deletion mutants aa1-50 and aa51-100. (G) Subcellular localizations of deletion mutants aa101-150 and aa291-318. The nuclei were stained with DAPI (A to G). (H) COS-7 cells were transfected with EYFP-BFLF2(101-150) or EYFP-BFLF2(291-318) for 24 h, then transfected cells were subjected to the interspecific heterokaryon assay. DAPI staining and cycloheximide treatment were performed. Mouse NIH3T3 cells were identified by their speckled nuclei when stained with DAPI (the red arrowhead). Each image is representative of the vast majority of the cells observed. Light-translucent pictures show the cellular morphology.

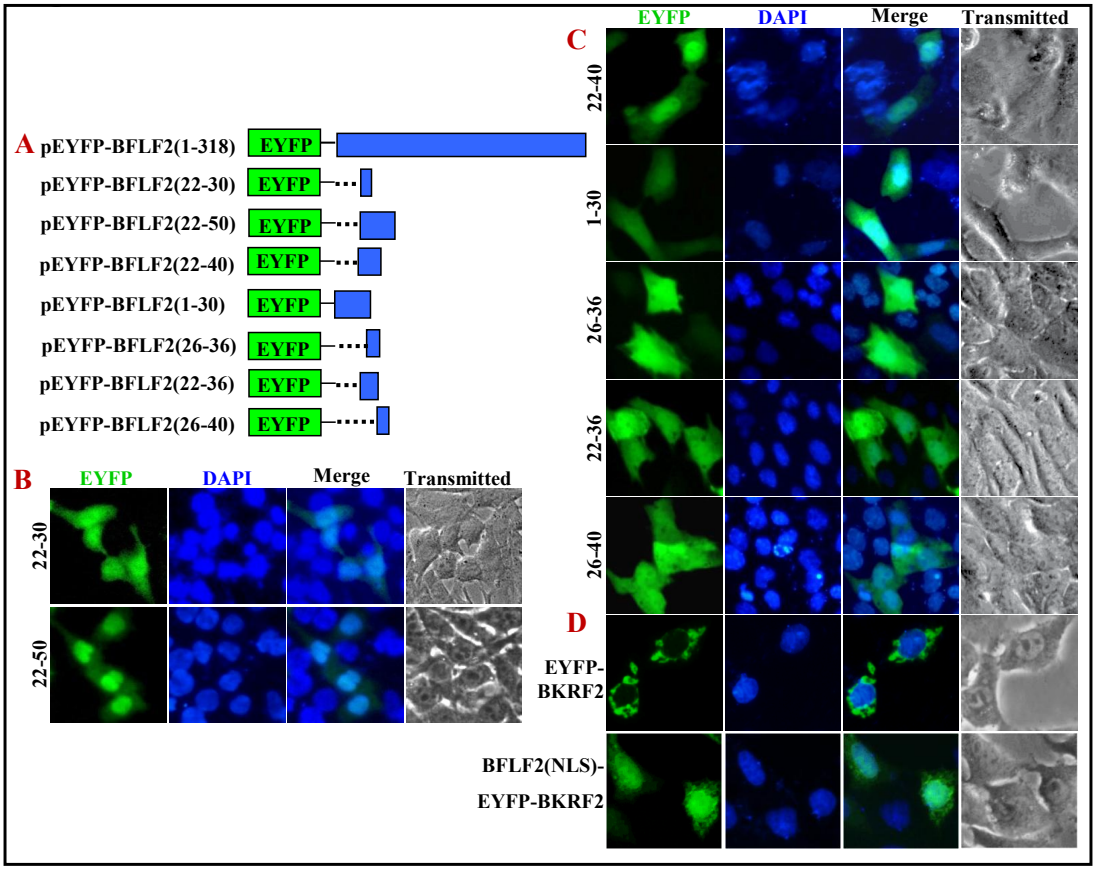

Fig. 3. aa22-40 of BFLF2 acts as the functional NLS. (A) Schematic representation of BFLF2 deletion mutants fused to the C-terminus of EYFP. (B) Subcellular localizations of deletion mutants aa22-30 and aa22-50. (C) Subcellular localizations of deletion mutants aa22-40, aa1-30, aa22-36, aa26-36 and aa26-40. (D) Subcellular localizations of EYFP-BKRF2 and BFLF2(NLS)-EYFP-BKRF2. The nuclei were stained with DAPI (B to D). Each image is representative of the vast majority of the cells observed. Light-translucent pictures show the cellular morphology.

Characterization of the functional NLS of BFLF2

To further identify the minimum sequence of BFLF2 for its nuclear localization, a series of deletion mutants (aa22-30, aa22-50, aa22-40 and aa1-30) were constructed (Fig. 3A). As results, aa22-30 located throughout the whole cell, while aa22-50 showed mainly nuclear localization (Fig. 3B), suggesting that aa22-50 (^{22}RRLMHPHHRNYTASKASAHSVKSVSRCGK^{50}), but not the predicted NLS aa22-30 (^{22}RRLMHPHHR^{30}), contained functional NLS. Furthermore, aa22-40 showed similar subcellular distribution with aa22-50 (Fig. 3C), indicating that aa22-40 might be the bona fide NLS of BFLF2. Nevertheless, aa1-30 showed pan-cellular localization, demonstrating aa12-30 from aa1-30 did not contain functional NLS, in turn confirmed that aa31-40 was important for NLS, and the basic aa 12 and 15 were not essential for the nuclear localization of BFLF2.

In order to test this speculation, three deletion mutants aa22-36, aa26-36 and aa26-40 were constructed (Fig. 3A) and transfected into COS-7 cells. As shown in Fig. 3, aa22-36, aa26-36 and aa26-40 all exhibited similar subcellular distribution patterns with EYFP, accumulated evenly in the cytoplasm and nucleus (Fig. 3C), indicating that aa22-25 and aa37-40 had a role in the nuclear localization of BFLF2, and aa22-40 was a genuine functional NLS. Simultaneously, the key aa for BFLF2 NLS might be ^{22}RR^{23}, ^{22}RRLMHPHHR^{30}, ^{28}HHR^{30} or ^{40}H.

To further prove aa22-40 was a genuine functional NLS, BFLF2 NLS(aa22-40) was fused with a absolutely cytoplasmic protein, EYFP-BKRF2 [3], to create pBFLF2(NLS)-EYFP-BKRF2 and then transfected into the cell for localization. As shown in Fig. 3D, EYFP-BKRF2 showed intense perinuclear subcellular localization, whereas the BFLF2(NLS)-EYFP-BKRF2 fusion protein could obviously be accumulated in the nucleus under the help of BFLF2 NLS. These results indicated that BFLF2 NLS can translocate the cytoplasmic protein to the nucleus, and aa22-40 is a genuine functional NLS.

Point mutations in NLS of BFLF2 identify the key aa

To identify the key aa in the functional NLS of BFLF2, basic aa within ^{22}RR^{23}, ^{22}RRLMHPHHR^{30}, ^{28}HHR^{30} or ^{40}H was mutated to alanine to construct BFLF2(22-23m), BFLF2(40m), BFLF2(22-30m) and BFLF2(28-30m) (Fig. 4A). When expressed in COS-7 cells, BFLF2(22-23m) showed primarily nuclear localization, but the cytoplasmic fluorescence was much more than that of EYFP-BFLF2 (Fig. 4B), indicating that ^{22}RR^{23} was the key aa and played partial role for the BFLF2 NLS. However, EYFP-BFLF2(40m) showed the same nuclear localization with EYFP-BFLF2 (Fig. 4B), suggesting that ^{40}H was not the key aa of BFLF2 NLS. When the mutation of aa22-23 was extended to aa22-30, BFLF2(22-30m) was distributed diffusely throughout the cells (Fig. 4B), suggesting ^{28}HHR^{30} might be the key aa of BFLF2 NLS. Not surprising, BFLF2(28-30m) showed similar subcellular localization pattern with that of BFLF2(22-23m) (Fig. 4B), strongly indicating that ^{28}HHR^{30} also was the key aa and took partial role for the BFLF2 NLS.

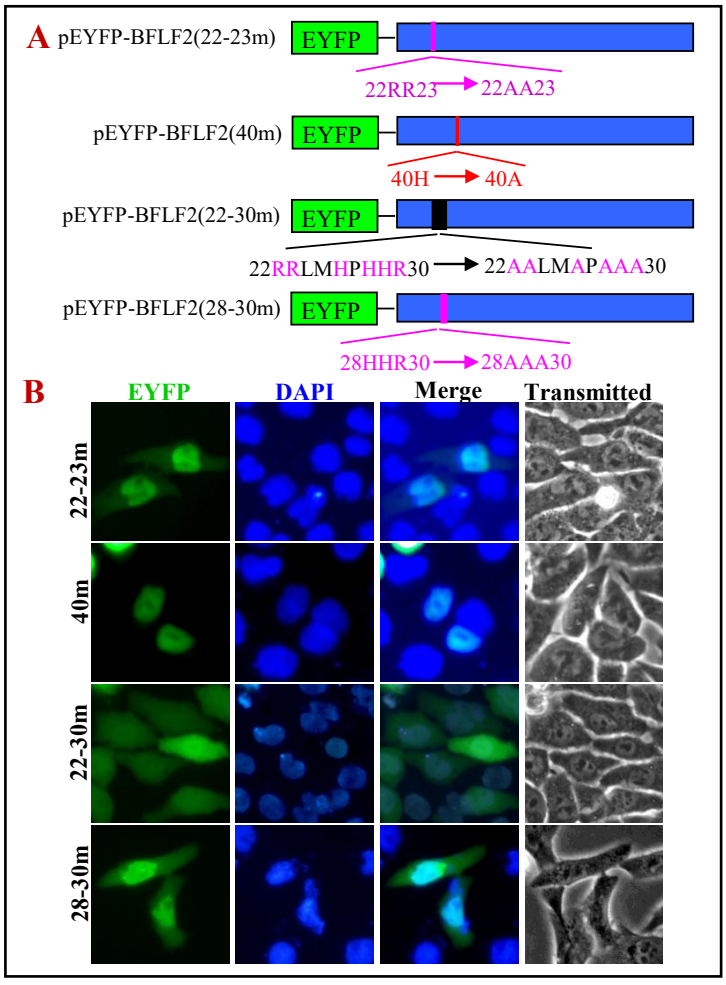

Fig. 4. Identification of the key aa of BFLF2 NLS. (A) Schematic representation of BFLF2 deletion mutants fused to the C-terminus of EYFP. (B) Subcellular localizations of deletion mutants BFLF2(22-23m), BFLF2(40m), BFLF2(22-30m) and BFLF2(28-30m). The nuclei were stained with DAPI. Each image is representative of the vast majority of the cells observed. Light-translucent pictures show the cellular morphology.

These results suggested that the predicted NLSs, NLS1 (^{22}RRLMHPHHR^{30}) and NLS2 (^{71}RHTRH^{75}), were insufficient for the nuclear localization of BFLF2, but the peptide sequence ^{22}RRLMHPHHRNYTASKASAH^{40} is the genuine functional NLS that is pivotal for the nuclear localization of BFLF2, and aa22-25 and aa37-40 are important aa sequences for its nuclear import. Besides, aa22-23 and aa28-30 are the key aa and play a role for the BFLF2 NLS.

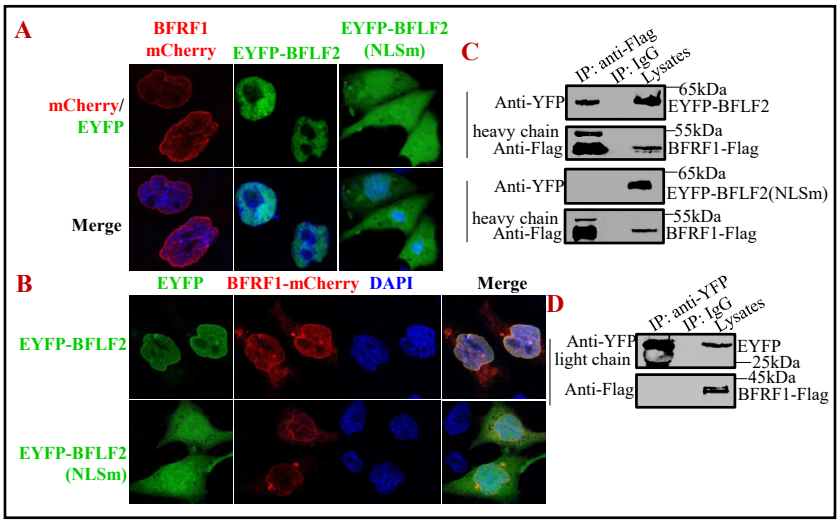

Fig. 5. The NLS of BFLF2 is involved in the interaction of BFLF2 and BFRF1. (A) Confocal microscopy of COS-7 cells transfected pBFRF1-mCherry, pEYFP-BFLF2 or pEYFP-BFLF2(NLSm) for 24 h. (B) Confocal microscopy of COS-7 cells co-transfected with plasmids pBFRF1-mCherry and pEYFP-BFLF2 or pEYFP-BFLF2(NLSm) for 24 h. The nuclei were stained with DAPI (A and B). All the photomicrographs were taken under a magnification of 630×. Each image is representative of the vast majority of the cells observed. (C) Co-IP analysis of pBFRF1-Flag and pEYFP-BFLF2, pBFRF1-Flag and pEYFP-BFLF2(NLSm). (D) Co-IP of BFRF1-Flag and control EYFP vector. HEK293T cells were co-transfected with plasmids combination pBFRF1-Flag/pEYFP-BFLF2, pBFRF1-Flag/pEYFP-BFLF2(NLSm) or pBFRF1-Flag/pEYFP-C1. 30 h post-transfection, cells were lysed and immunoprecipitated with anti-Flag mAb (C) or anti-YFP pAb (D) or mouse IgG control. Immunoprecipitated proteins as well as the cell lysates were separated in denaturing 10% SDS-PAGE, and analyzed by IB with anti-Flag mAb or anti-YFP pAb.

The BFLF2 NLS is involved in the interaction between BFLF2 and BFRF1

Previous study demonstrates that BFLF2 expression is strictly connected with the expression of BFRF1 [16], which normally binds and anchors BFLF2 on the nuclear membrane, but BFLF2 has no obvious influence on the intracellular localization of BFRF1 [18]. In order to explore whether the BFLF2 NLS is participated in the BFLF2 and BFRF1 interaction, COS-7 cells were transiently co-transfected BFRF1-mCherry either with EYFP-BFLF2 or EYFP-BFLF2(NLSm), namely EYFP-BFLF2(22-30m). As controls, these plasmids were also transfected alone into COS-7 cells. As shown in Fig. 5, BFRF1-mCherry expressed alone was located predominantly at the nuclear envelope and partial near the perinuclear, which looks like cytoplasmic structure (Fig. 5A). Upon co-expression of BFRF1-mCherry with EYFP-BFLF2, EYFP-BFLF2 was exclusively targeted to the nuclear envelope. While co-expression of BFRF1-mCherry with EYFP-BFLF2 (NLSm), EYFP-BFLF2 (NLSm) was localized evenly in the cytoplasm and nucleus (Fig. 5B), indicating BFLF2 NLS may be involved in the interaction between BFLF2 and BFRF1.

To further verify this speculation, BFRF1-Flag was either co-transfected with EYFP-BFLF2 or EYFP-BFLF2(NLSm) expressing plasmid, and Co-IP experiments were carried out with anti-Flag mAb. As results, BFLF2, but not BFLF2(NLSm), could be immunoprecipitated by BFRF1 (Fig. 5C). As control, no target protein was immunoprecipitated by the negative control mouse IgG or EYFP protein (Fig. 5C and 5D). These results indicated that BFLF2 NLS is involved in the BFLF2 and BFRF1 interaction, which can regulate the nuclear membrane localization of BFLF2.

The nuclear export of BFLF2 is independent of CRM1

CRM1 is a nuclear export receptor for both U snRNAs and proteins like Rev that carry a leucine-rich NES [42]. Conversely, LMB, a cytotoxin that is shown to bind to CRM1, specifically inhibits the nuclear export of Rev and U snRNAs [42]. To address the question of whether the nuclear export of BFLF2 is dependent on CRM1, COS-7 cells were transiently transfected with pEYFP-BFLF2 or the control pEYFP-UL6 (HSV-1) or pEYFP-UL54 (PRV), which is

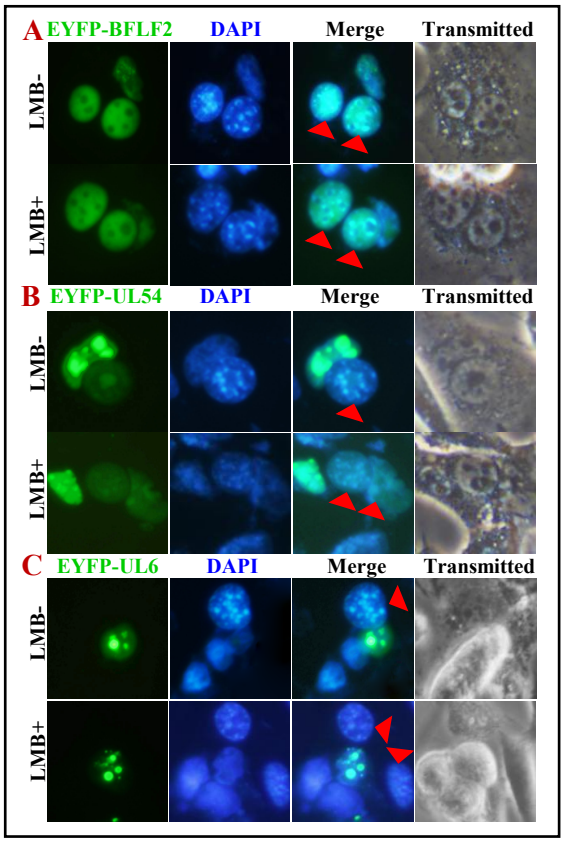

Fig. 6. CRM1 is not the nuclear export receptor of BFLF2. COS-7 cells were transiently transfected with pEYFP-BFLF2 (A), pEYFP-UL54 (B) or pEYFP-UL6 (C), 18 h post-transfection, mouse NIH3T3 cells were plated on to the COS-7 cells in a medium containing cycloheximide (50 μg/mL) in the absence or presence of LMB (20 ng/mL). After 4 h, the cells were washed with PBS and fused by the addition of 2 mL of 50% PEG in PBS. After washing, the cells were returned to a medium containing cycloheximide in the absence or presence of LMB for 1h. Mouse cells were identified by their speckled nuclei when stained with 0.5 μg/mL DAPI dye (the red arrowhead). Each image is representative of the vast majority of the cells observed. Light-translucent pictures show the cellular morphology.

shown to export from the nucleus to the cytoplasm independent of CRM1 [32]. At 18 h post-transfection, COS-7 cells were fused with an equivalent number of mouse NIH3T3 cells in the presence of cycloheximide, together culturing for 4 h. Protein synthesis was blocked with 50 μg/mL cycloheximide 30 min prior to fusion and throughout the experiment. Besides, the cells were treated with or without LMB at 20 ng/mL 3 h before cell fusion, to inhibit the function of CRM1.

As shown in Fig. 6, EYFP-BFLF2 and EYFP-UL54 were detected in both monkey and mouse cell nuclei in the absence of LMB (Fig. 6A and 6B). In contrast, EYFP-UL6 could not be detected in mouse cell nuclei (Fig. 6C), indicating that BFLF2, but not UL6, has the ability to shuttle in different cells. In addition, similar results were observed in the presence of LMB, suggesting that BFLF2 can shuttle between the nucleus and cytoplasm through a CRM-1-independent pathway.

The nuclear export of BFLF2 is mediated through TAP/NXF1-dependent pathway

It's reported that cells can make use of multiple transport systems to transport RNAs and proteins from the nucleus to cytoplasm [32], and TAP/NXF1 has been shown to implicate in the export of protein and mRNA [43]. Therefore, to explore whether TAP is involved in the nuclear export of BFLF2, EYFP-BFLF2 and TAP-mCherry expressing plasmids were firstly co-transfected into COS-7 cells. As a result, EYFP-BFLF2 was significantly redistributed from the nucleus to cytoplasm (Fig. 7A and 7B), indicating that TAP/NXF1 may be important for the nuclear export of BFLF2. To further confirm the association between BFLF2 and TAP, Co-IP was performed. HEK293T cells were co-transfected either with plasmids combination pEYFP-BFLF2/pFLAG-CMV-TAP or negative control pEYFP-BFLF2/pCMV-Flag and pEYFP-C1/pFLAG-CMV-TAP. After transfection for 30 h, cell lysates were collected and immunoprecipitated with anti-Flag mAb or mouse IgG. As shown in Fig. 7, FLAG-TAP was clearly shown to co-immunoprecipitate with EYFP-BFLF2 (Fig. 7C). As negative controls,

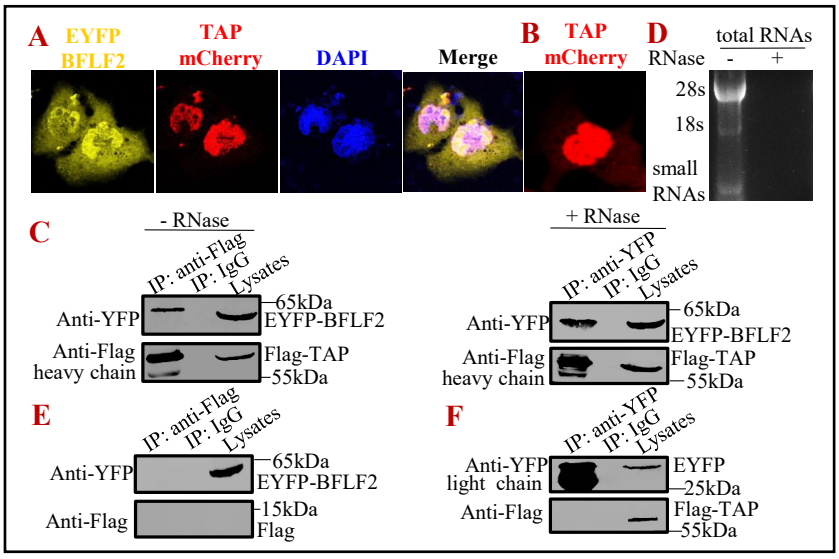

Fig. 7. Identification of the nuclear export mechanism of BFLF2. (A) TAP promotes the nuclear export of BFLF2. COS-7 cells were co-transfected with pEYFP-BFLF2 and pTAP-mCherry. The nuclei were stained with DAPI. (B) Subcellular localization of TAP-mCherry transfected COS-7 cells. (C) Co-IP analysis of EYFP-BFLF2 and FLAG-CMV-TAP expressing plasmids co-transfected HEK293T cells after treatment with or without RNase A at 150 μg/mL. (D) Confirmation of efficient RNase treatment. Total RNA of HEK293T cells was incubated for 30 min at 37 °C in the absence (−) or presence (+) of 150 μg/mL RNase. The RNase condition was used in all experiments. (E) Co-IP of EYFP-BFLF2 and control Flag vector. (F) Co-IP of FLAG-CMV-TAP and control EYFP vector. HEK293T cells were co-transfected with plasmids combination pCMV-Flag/pEYFP-BFLF2 (E), pEYFP-BFLF2/pFLAG-CMV-TAP (C) or pEYFP/pFLAG-CMV-TAP (F). 30 h post-transfection, cells were lysed and IP with anti-Flag mAb or anti-YFP pAb or mouse IgG control. Immunoprecipitated proteins as well as the cell lysates were separated in denaturing 10% SDS-PAGE, and analyzed by IB with anti-Flag mAb or anti-YFP pAb.

EYFP-BFLF2 was not co-immunoprecipitated by anti-Flag from cells co-expressing EYFP-BFLF2 and CMV-Flag (Fig. 7E), and FLAG-CMV-TAP was not co-immunoprecipitated by anti-YFP from cells co-expressing FLAG-CMV-TAP and pEYFP-C1 (Fig. 7F).

The above positive Co-IP results might not be due to direct interaction but rather in a tertiary complex with RNAs [32], since TAP is a RNA binding protein [44]. In order to investigate whether the interaction between BFLF2 and TAP is associated with RNA, lysates from cells co-transfected with BFLF2 and TAP proteins were treated with RNase prior to immunoprecipitation, and result showed the amounts of co-immunoprecipitated TAP with BFLF2 remained substantially unchanged after RNase treatment (Fig. 7C), confirming RNA was not involved in the interaction between BFLF2 and TAP. These results suggested that the nuclear export of BFLF2 depended on TAP without RNA participation.

Mechanisms of the nuclear import of BFLF2

Transport of proteins into the nucleus is mediated by soluble receptor proteins that interact with nuclear cargo and carry it through the nuclear pore [45]. Importin α recognizes cargo proteins with a NLS, while importin β binds and ferries the complex into the nucleus, and the small regulatory GTPase Ran binds to importin β and dissociates the complex to complete the import [46]. To explore whether Ran is required for the nuclear import of BFLF2, a DN RanGTP (Ran-Q69L), which lacks the ability in GTP hydrolysis [47], was used. Compared to the negative control (Fig. 8A), the nuclear import of BFLF2 in cells co-transfected with pEYFP-BFLF2 and pRan-Q69L-mCherry for 24 h was significantly blocked (Fig. 8B), indicating that the nuclear translocation of BFLF2 is Ran-dependent and requires Ran GTP hydrolysis.

In mammals, there are at least six isoforms of karyopherins-α, including importin α1, importin α3, importin α4, importin α5, importin α6 and importin α7 [46, 48]. Moreover,

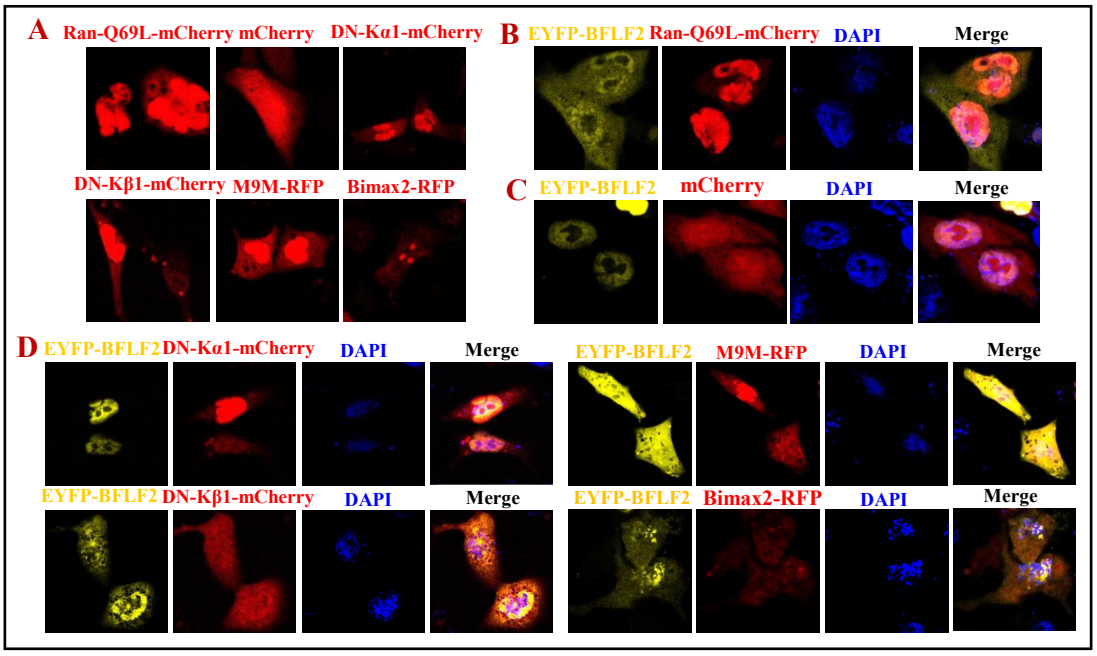

Fig. 8. The nuclear import mechanisms of BFLF2. (A) Confocal microscopy of COS-7 cells transfected with Ran-Q69L-mCherry, DN kα1-mCherry, DN kβ1-mCherry, M9M-RFP, Bimax2-RFP or mCherry for 24 h. (B) Confocal microscopy of COS-7 cells co-transfected with plasmids pEYFP-BFLF2 and pRan-Q69L-mCherry. (C) Confocal microscopy of COS-7 cells co-transfected with pEYFP-BFLF2 and pmCherry-N1. (D) Confocal microscopy of COS-7 cells co-transfected with plasmid pEYFP-BFLF2 and plasmid encoding DN kα1-mCherry, DN kβ1-mCherry, M9M-RFP or Bimax2-RFP. The nuclei were stained with DAPI (B to D). All the photomicrographs were taken under a magnification of 630×. Each image is representative of the vast majority of the cells observed.

several importin β members could directly recognize NLSs, especially the extensively studied importin β1 and importin β2 (transportin-1) [49]. In order to determine the nuclear transport receptors of BFLF2, DN importin α5 (also called kα1, lacks the ability to bind importin β) [26, 50] and DN importin β1 (also called kβ1, lacks the ability to bind Ran) [50, 51], nuclear transport inhibitors M9M (competes effectively with wild-type NLS and binds specifically to transportin-1 [52]) and Bimax2 (severely inhibits the members of importin α, including importin α1, α3 and α7 [53]), were introduced. In constrast to the negative control (Fig. 8A), BFLF2 was not relocalized by mCherry (Fig. 8C), but DN kβ1, M9M and Bimax2 could damage the nuclear accumulation of BFLF2, and leaded to the fluorescence accumulation in cytoplasm, while DN kα1 could not change the subcellular localization of BFLF2 (Fig. 8D). These results demonstrated that BFLF2 may be transported into nucleus by importin β1, transportin-1 and at least one of proteins from importin α1, α3 and α7.

To further confirm the hypothesis mentioned above, HEK293T cells were co-transfected pEYFP-BFLF2 with either of the following plasmid: pcDNA-Flag-kα1, pFlag-kα2, pFlag-kα4, pFlag-kα6, pCMV9-3×Flag-importinβ1 or pFlag-CMV-transportin-1. At 30 h post-transfection, cell lysates were prepared and Co-IP was carried out using anti-Flag mAb or mouse IgG. Immunoprecipitated proteins were subjected to IB analysis with Flag or YFP antibody. As results, BFLF2 was efficiently co-immunoprecipitated with kα6 (Fig. 9A), importin β1 (Fig. 9B) and transportin-1 (Fig. 9C), but not kα1 (Fig. 9D), kα2 (Fig. 9E) or kα4 (Fig. 9F). As control, no target protein was immunoprecipitated by IgG (Fig. 9), indicating BFLF2 was associated with importin α7, importin β1 and transportin-1. To exclude the interactions of EYFP with importin α7, importin β1 and transportin-1, plasmids combination pFlag-kα6/pEYFP-C1, pCMV9-3×Flag-importinβ1/pEYFP-C1, pCMV-Flag-transportin-1/pEYFP-C1 or pEYFP-BFLF2/pCMV-Flag-N1 were co-transfected into HEK293T cells, then Co-IP was

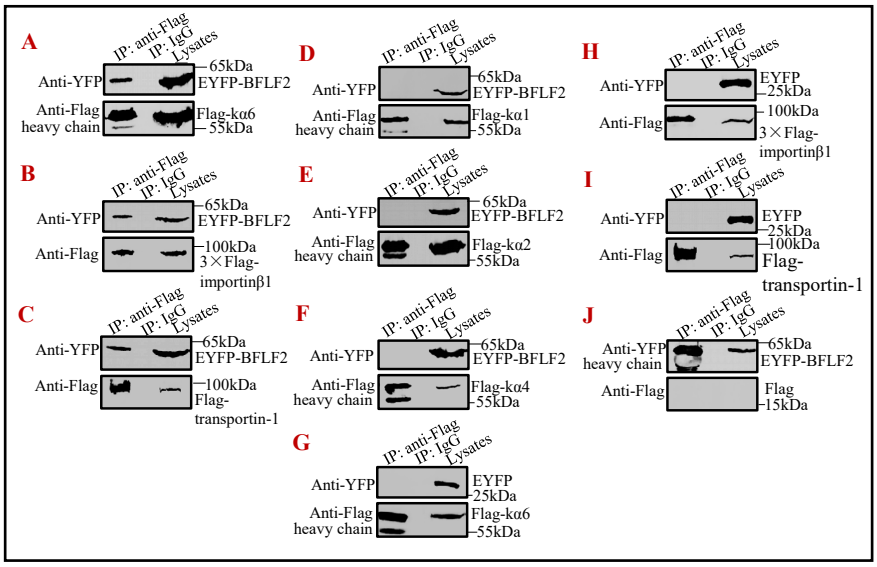

Fig. 9. Verification of the interactions between BFLF2 and importin α1, importin α3, importin α5 importin α7, importin β1 or transportin-1. Co-IP of BFLF2 with importin α7 (kα6) (A), importin β1 (B), transportin-1 (C), importin α5 (kα1) (D), importin α1 (kα2) (E) or importin α3 (kα4) (F). HEK293T cells were co-transected with pEYFP-BFLF2 and pcDNA-Flag-kα1 (Flag-kα1), pFlag-kα2, pFlag-kα4, pFlag-kα6, pCMV9-3×Flag-importin β1 (3×Flag-importin β1) or pFLAG-CMV-transportin-1 (Flag-transportin-1). 30 h post-transfection, cells were lysed and IP with anti-Flag or mouse IgG control. Immunoprecipitated proteins as well as the cell lysates were separated in denaturing 10% SDS-PAGE, and analyzed by IB with anti-Flag mAb or anti-YFP pAb. Besides, Co-IP were also performed on the lysates of negative control pFlag-kα6/pEYFP-C1 (G), pCMV9-3×Flag-importin β1/pEYFP-C1 (H), pFLAG-CMV-transportin-1/pEYFP-C1 (I) or pEYFP-BFLF2/pCMV-Flag (J) co-transfected HEK293T cells.

performed. As shown in Fig. 9, no EYFP protein was immunoprecipitated by anti-Flag mAb (Fig. 9G, 9H and 9I), suggesting that EYFP couldn't interact with importin α7, importinβ1 or transportin-1. Besides, no protein was immunoprecipitated by EYFP-BFLF2 using anti-YFP (Fig. 9J), proving that BFLF2 can interact with the nuclear import receptors importin α7, importin β1 and transportin-1, but not importin α1, α3 or α5.

BFLF2 binds TAP/NXF1, importin α7, importin β1 and transportin-1 in EBV-infected cells

In order to explore the physiological mechanisms of EBV natural hosting cells, the EBV-latent cells (HONE1-EBV cells), which were generated by infecting human gastric adenocarcinoma cells (AGS) and HONE1 cells with recombinant EBV genomes expressing GFP [21, 54], were chosen to continue the experiments. HONE1-EBV cells were transfected with expressing plasmid pFLAG-CMV-TAP, pCMV9-3×Flag-importin β1, pFlag-kα6, pFLAG-CMV-transportin-1 or pFLAG-CMV-2, and cells were induced to undergo lytic cycle activation by transfecting with pBZLF1-HA plasmid. Subsequently, cells were collected and Co-IP was performed using anti-Flag mAb. As results, BFLF2 could be immunoprecipitated by TAP/NXF1 (Fig. 10A), importin α7 (Fig. 10B), importin β1 (Fig. 10C) and transportin-1(Fig. 10D), but not the Flag-vector control (Fig. 10E), demonstrating that BFLF2 can interact with TAP/NXF1, importin α7, importin β1 and transportin-1 during EBV infection.

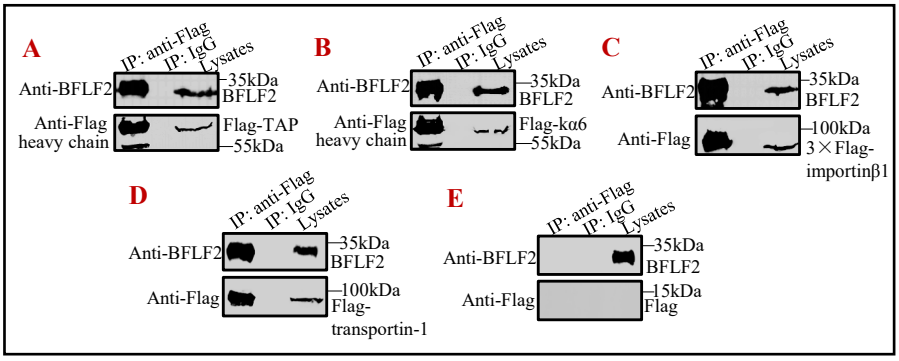

Fig. 10. BFLF2 binds TAP/NXF1, importin α7, importin β1 and transportin-1 in HONE1-EBV cells. Co-IP of BFLF2 with TAP/NXF1 (A), importin α7 (kα6) (B), importin β1 (C), transportin-1 (D) or Flag-vector control (E). HONE1-EBV cells were transfected with the indicated expression plasmid pFLAG-CMV-TAP, pCMV9-3×Flag-importin β1, pFlag-kα6, pFLAG-CMV-transportin-1 or pFLAG-CMV-2, respectively. 12 h post-transfection, cells were transfected with pBZLF1-HA to induce the lytic replication of EBV for 24 h. Then cells were lysed and IP with anti-Flag mAb or mouse IgG control. Immunoprecipitated proteins as well as the cell lysates were separated in denaturing 10% SDS-PAGE, and analyzed by IB with anti-BFLF2 pAb or anti-Flag mAb.

Discussion

HSV-1 UL31 protein is a multi-functional nucleoprotein, which is transported into the nucleus via Ran-, transportin-1- and importin α1-mediated pathway [19], and this nuclear accumulation is important for viral infection [55]. Meanwhile, HSV-1 UL31 and its homologue EBV BFLF2 are both crucial for efficient viral DNA packaging and primary egress across the nuclear membrane [18]. Therefore, it prompts us to identify the transport mechanisms of BFLF2.

Nucleocytoplasmic shuttling protein needs NLS and NES. We showed that BFLF2 can shuttle between the nucleus and cytoplasm. In consideration of BFLF2 contains two leucine-rich motifs that resemble the HIV Rev NES [56], we suspected that the predicted leucine-rich NESs (Fig. 2B) might play a vital role in the nuclear export of BFLF2 [57]. However, we failed to find the functional NES, since mutations of predicted NES1 and NES2 did not impact the ability of BFLF2 to shuttle from the nucleus to cytoplasm (Fig. 2H), which might be due to the space folding of BFLF2, and therefore the functional NES cannot be exposed. However, we confirmed that the nuclear export of BFLF2 occurs not through its interaction with CRM1, but through the TAP export pathway without RNA participation, this was consistent with the nuclear export of HSV-1 ICP27, herpesvirus saimiri ORF57 and PRV UL54 (Fig. 11C) [32, 58].

As schematically represented in Fig. 11A, one newly characterized NLS containing basic aa clusters was found to be responsible for the nuclear localization of BFLF2. After a series of mutation analysis and fluorescence microscopy, ^{22}RRLMHPHHRNYTASKASAH^{40} was identified as the functional NLS of BFLF2, and aa22-23 and aa28-30 were the crucial aa for its nuclear localization.

In the course of evolution, virus is generally conservative and only few genes will undergo mutation. Thus, the viral evolution can be investigated at the molecular level. Multiple amino acid sequence alignments of EBV BFLF2 and its homologues showed that EBV BFLF2 had a relatively low homology with HSV-1 UL31 (20%), KSHV ORF69 (34%) and VZV ORF27 (21%), respectively (Fig. 11B). Although EBV BFLF2 and HSV-1 UL31 possess functional NLS and predicted NES [19], the NLS and NES of KSHV ORF69 and VZV ORF27 currently did not reported or could not be predicted by bioinformatic analysis, the NLS and NES alignments of EBV BFLF2, HSV-1 UL31, KSHV ORF69 and VZV ORF27 were therefore could not be carried out. Consequently, we infered the identified/putative NLSs and NESs of EBV BFLF2 and its homologues were not conserved, and this conclusion needed to be verified in the future.

Active nucleocytoplasmic transport of certain protein is dependent on a gradient of Ran-GTP across the nuclear membrane, which is mediated by importin α to recognize the

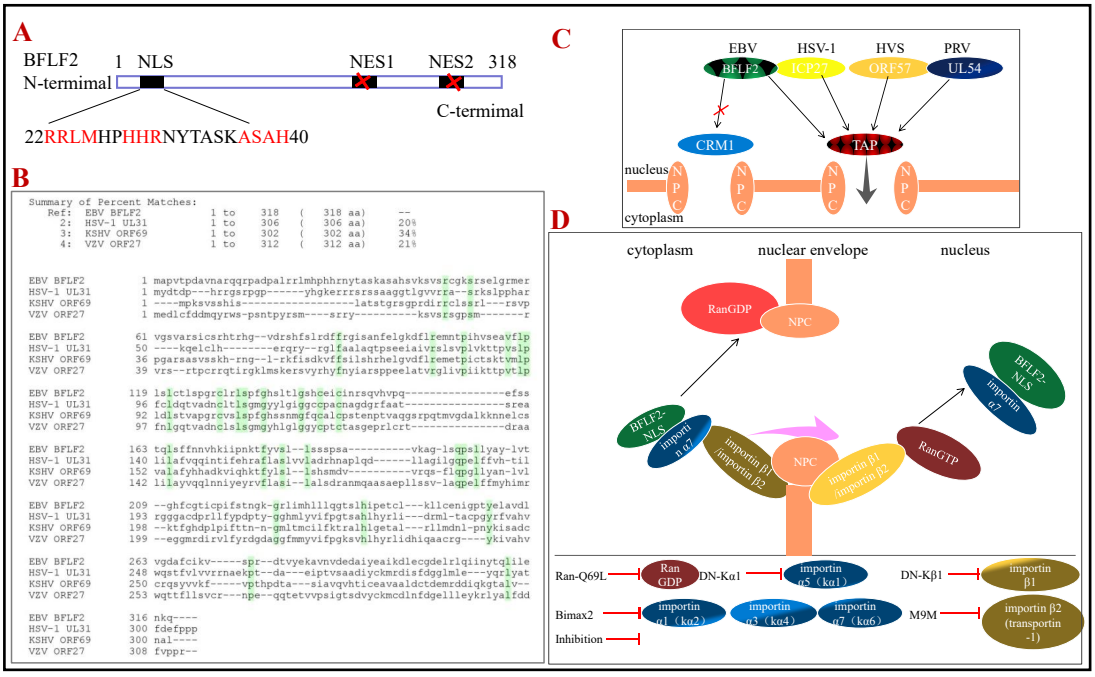

Fig. 11. Schematic diagram of the subcellular transport mechanisms of BFLF2. (A) Schematic diagram of the aa sequences of the identified NLS and predicted NES1 and NES2 within BFLF2. (B) Multiple aa sequence alignment of EBV BFLF2 and its homologues HSV-1 UL31, KSHV ORF69 and VZV ORF27, using Clone Manager software (Version 8.0). Green colors indicate the identical aa among EBV BFLF2, HSV-1 UL31, KSHV ORF69 and VZV ORF27. (C) Schematic diagram of the nuclear export of BFLF2 via TAP-dependent pathway. (D) Schematic diagram of the nuclear import mechanisms of BFLF2.

NLS and importin β to promote the importin α-NLS interplay [59, 60]. Expectedly, our study demonstrated that the nuclear transport of BFLF2 protein was abolished by Ran-Q69L, indicating that BFLF2 is a Ran-dependent protein and is transported into the nucleus from cytoplasm via a classical nuclear transport machinery.

Besides, DN kβ1, DN kα1 and inhibitors Bimax2 and M9M were employed, our results showed that DN kβ1, Bimax2 and M9M impaired the nuclear transport of BFLF2, suggesting that the nuclear transport of BFLF2 may be mediated by importin β1, transportin-1 and at least one of the transport receptor importin α1, α3 or α7. To further verify this result, Co-IP assays were performed and showed that BFLF2 could interact with importin α7, importin β1 and transportin-1 in transiently transfected HEK293T cells and EBV-latent cells.

Conclusion

Taken together, we here demonstrated that BFLF2 is a nucleocytoplasmic trafficking protein. In addition, BFLF2 shuttles between the nucleus and cytoplasm through TAP-dependent nuclear export pathway (independent of RNA) and through Ran-, importin α7-, importin β1- and transportin-1-dependent nuclear import mechanism (Fig. 11C and 11D). These results would uncover the molecular mechanisms for nucleocytoplasmic shuttling of BFLF2 and open up new avenues toward delineating its biological functions during EBV infection.

Acknowledgements

This work was supported by grants from the National Natural Science Foundation of China (81772179, 31400150 and 31200120); the Natural Science Foundation of

Guangdong Province (2018A0303130257 and 2015A030313473); the Training Program for Outstanding Young Teachers in Universities of Guangdong Province (YQ2015132); the Medical Scientific Research Foundation of Guangdong Province, China (A2017055 and B2012165); the Guangzhou Innovation Leading Team Program (#CYLJTD-201602); the Science and Technology Plan Projects of Guangzhou City, China (201607010088); the Scientific Research Projects in Colleges and Universities of Guangzhou (1201430024, 1201610025 and 1201610024); Innovation and entrepreneurship training program in colleges and universities in Guangzhou (2017224104); High-Level Universities Academic Backbone Development Program of Guangzhou Medical University; Thousand Hundred Ten Projects of Guangzhou Medical University, Guangdong; and the Provincial Training Programs of Innovation and Entrepreneur-ship for Undergraduates in Guangzhou Medical University (201710570070).

Disclosure Statement

The authors confirm that they have no conflicts of interest.

References

1 Stanfield BA, Luftig MA: Recent advances in understanding Epstein-Barr virus. F1000Res 2017;6:386.
2 Kenney SC, Mertz JE: Regulation of the latent-lytic switch in Epstein-Barr virus. Semin Cancer Biol 2014;26:60-68.
3 Cai M, Liao Z, Chen T, Wang P, Zou X, Wang Y, Xu Z, Jiang S, Huang J, Chen D, Peng T, Hong G, Li M: Characterization of the subcellular localization of Epstein-Barr virus encoded proteins in live cells. Oncotarget 2017;8:70006-70034.
4 Tarbouriech N, Buisson M, Geoui T, Daenke S, Cusack S, Burmeister WP: Structural genomics of the Epstein-Barr virus. Acta Crystallogr D Biol Crystallogr 2006;62:1276-1285.
5 Kuss SK, Mata MA, Zhang L, Fontoura BM: Nuclear imprisonment: viral strategies to arrest host mRNA nuclear export. Viruses 2013;5:1824-1849.
6 Gorlich D, Mattaj IW: Nucleocytoplasmic transport. Science 1996;271:1513-1518.
7 Chen IH, Sciabica KS, Sandri-Goldin RM: ICP27 interacts with the RNA export factor Aly/REF to direct herpes simplex virus type 1 intronless mRNAs to the TAP export pathway. J Virol 2002;76:12877-12889.
8 Bachi A, Braun IC, Rodrigues JP, Pante N, Ribbeck K, von Kobbe C, Kutay U, Wilm M, Gorlich D, Carmo-Fonseca M, Izaurralde E: The C-terminal domain of TAP interacts with the nuclear pore complex and promotes export of specific CTE-bearing RNA substrates. RNA 2000;6:136-158.
9 Gorlich D, Dabrowski M, Bischoff FR, Kutay U, Bork P, Hartmann E, Prehn S, Izaurralde E: A novel class of RanGTP binding proteins. J Cell Biol 1997;138:65-80.
10 Gorlich D: Nuclear protein import. Curr Opin Cell Biol 1997;9:412-419.
11 Popa M, Ruzsics Z, Lotzerich M, Dolken L, Buser C, Walther P, Koszinowski UH: Dominant negative mutants of the murine cytomegalovirus M53 gene block nuclear egress and inhibit capsid maturation. J Virol 2010;84:9035-9046.
12 Guan Y, Guo L, Yang E, Liao Y, Liu L, Che Y, Zhang Y, Wang L, Wang J, Li Q: HSV-1 nucleocapsid egress mediated by UL31 in association with UL34 is impeded by cellular transmembrane protein 140. Virology 2014;464-465:1-10.
13 Bailer SM, Haas J: Connecting viral with cellular interactomes. Curr Opin Microbiol 2009;12:453-459.
14 Desai PJ, Pryce EN, Henson BW, Luitweiler EM, Cothran J: Reconstitution of the Kaposi's sarcoma-associated herpesvirus nuclear egress complex and formation of nuclear membrane vesicles by coexpression of ORF67 and ORF69 gene products. J Virol 2012;86:594-598.
15 Farina A, Santarelli R, Bloise R, Gonnella R, Granato M, Bei R, Modesti A, Cirone M, Bengtsson L, Angeloni A, Faggioni A: KSHV ORF67 encoded lytic protein localizes on the nuclear membrane and alters emerin distribution. Virus Res. 2013;175:143-150.
16 Gonnella R, Farina A, Santarelli R, Raffa S, Feederle R, Bei R, Granato M, Modesti A, Frati L, Delecluse HJ, Torrisi MR, Angeloni A, Faggioni A: Characterization and intracellular localization of the Epstein-Barr virus protein BFLF2: interactions with BFRF1 and with the nuclear lamina. J Virol 2005;79:3713-3727.

17 Yadav S, Libotte F, Buono E, Valia S, Farina G, Faggioni A, Farina A: EBV early lytic protein BFRF1 alters emerin distribution and post-translational modification. Virus Res. 2017;232:113-122.
18 Granato M, Feederle R, Farina A, Gonnella R, Santarelli R, Hub B, Faggioni A, Delecluse HJ: Deletion of Epstein-Barr virus BFLF2 leads to impaired viral DNA packaging and primary egress as well as to the production of defective viral particles. J Virol 2008;82:4042-4051.
19 Cai M, Chen D, Zeng Z, Yang H, Jiang S, Li X, Mai J, Peng T, Li M: Characterization of the nuclear import signal of herpes simplex virus 1 UL31. Arch Virol 2016;161:2379-2385.
20 Cai M, Si J, Li X, Zeng Z, Li M: Characterization of the nuclear import mechanisms of HSV-1 UL31. Biol Chem 2016;397:555-561.
21 Lui VW, Wong EY, Ho Y, Hong B, Wong SC, Tao Q, Choi GC, Au TC, Ho K, Yau DM, Ma BB, Hui EP, Chan AS, Tsang CM, Tsao SW, Grandis JR, Chan AT: STAT3 activation contributes directly to Epstein-Barr virus-mediated invasiveness of nasopharyngeal cancer cells *in vitro*. Int J Cancer 2009;125:1884-1893.
22 Kanda T, Shibata S, Saito S, Murata T, Isomura H, Yoshiyama H, Takada K, Tsurumi T: Unexpected instability of family of repeats (FR), the critical cis-acting sequence required for EBV latent infection, in EBV-BAC systems. PLoS One 2011;6:e27758.
23 Cai M, Huang Z, Liao Z, Chen T, Wang P, Jiang S, Chen D, Peng T, Bian Y, Hong G, Yang H, Zeng Z, Li X, Li M: Characterization of the subcellular localization and nuclear import molecular mechanisms of herpes simplex virus 1 UL2. Biol Chem 2017;398:509-517.
24 Tanaka M, Kagawa H, Yamanashi Y, Sata T, Kawaguchi Y: Construction of an excisable bacterial artificial chromosome containing a full-length infectious clone of herpes simplex virus type 1: viruses reconstituted from the clone exhibit wild-type properties *in vitro* and *in vivo*. J Virol 2003;77:1382-1391.
25 Isegawa Y, Miyamoto Y, Yasuda Y, Semi K, Tsujimura K, Fukunaga R, Ohshima A, Horiguchi Y, Yoneda Y, Sugimoto N: Characterization of the human herpesvirus 6 U69 gene product and identification of its nuclear localization signal. J Virol 2008;82:710-718.
26 Reid SP, Valmas C, Martinez O, Sanchez FM, Basler CF: Ebola virus VP24 proteins inhibit the interaction of NPI-1 subfamily karyopherin alpha proteins with activated STAT1. J Virol 2007;81:13469-13477.
27 Guo H, Mao R, Block TM, Guo JT: Production and function of the cytoplasmic deproteinized relaxed circular DNA of hepadnaviruses. J Virol 2010;84:387-396.
28 Birbach A, Bailey ST, Ghosh S, Schmid JA: Cytosolic, nuclear and nucleolar localization signals determine subcellular distribution and activity of the NF-kappaB inducing kinase NIK. J Cell Sci 2004;117:3615-3624.
29 Kino Y, Washizu C, Aquilanti E, Okuno M, Kurosawa M, Yamada M, Doi H, Nukina N: Intracellular localization and splicing regulation of FUS/TLS are variably affected by amyotrophic lateral sclerosis-linked mutations. Nucleic Acids Res 2011;39:2781-2798.
30 Mizuguchi C, Moriyama T, Yoneda Y: Generation and characterization of a monoclonal antibody against importin alpha7/NPI-2. Hybridoma (Larchmt) 2011;30:307-309.
31 Depping R, Steinhoff A, Schindler SG, Friedrich B, Fagerlund R, Metzen E, Hartmann E, Kohler M: Nuclear translocation of hypoxia-inducible factors (HIFs): involvement of the classical importin alpha/beta pathway. Biochim Biophys Acta 2008;1783:394-404.
32 Li M, Wang S, Cai M, Guo H, Zheng C: Characterization of molecular determinants for nucleocytoplasmic shuttling of PRV UL54. Virology 2011;417:385-393.
33 Cai M, Wang S, Xing J, Zheng C: Characterization of the nuclear import and export signals, and subcellular transport mechanism of varicella-zoster virus ORF9. J Gen Virol 2011;92:621-626.
34 Cai M, Jiang S, Zeng Z, Li X, Mo C, Yang Y, Chen C, Xie P, Bian Y, Wang J, Huang J, Chen D, Peng T, Li M: Probing the nuclear import signal and nuclear transport molecular determinants of PRV ICP22. Cell Biosci 2016;6:3.
35 Borer RA, Lehner CF, Eppenberger HM, Nigg EA: Major nucleolar proteins shuttle between nucleus and cytoplasm. Cell 1989;56:379-390.
36 Pinol-Roma S, Dreyfuss G: Shuttling of pre-mRNA binding proteins between nucleus and cytoplasm. Nature 1992;355:730-732.
37 Zhu H, Zheng C, Xing J, Wang S, Li S, Lin R, Mossman KL: Varicella-zoster virus immediate-early protein ORF61 abrogates the IRF3-mediated innate immune response through degradation of activated IRF3. J Virol 2011;85:11079-11089.
38 Cai M, Li M, Wang K, Wang S, Lu Q, Yan J, Mossman KL, Lin R, Zheng C: The herpes simplex virus 1-encoded envelope glycoprotein B activates NF-kappaB through the Toll-like receptor 2 and MyD88/TRAF6-dependent signaling pathway. PLoS One 2013;8:e54586.

39 Li M, Jiang S, Mo C, Zeng Z, Li X, Chen C, Yang Y, Wang J, Huang J, Chen D, Peng T, Cai M: Identification of molecular determinants for the nuclear import of pseudorabies virus UL31. Arch Biochem Biophys 2015;587:12-17.
40 Liu C, Cheng A, Wang M, Chen S, Jia R, Zhu D, Liu M, Sun K, Yang Q, Chen X: Characterization of nucleocytoplasmic shuttling and intracellular localization signals in Duck Enteritis Virus UL54. Biochimie 2016;127:86-94.
41 Zheng C, Brownlie R, Babiuk LA, van Drunen Littel-van den Hurk S: Characterization of nuclear localization and export signals of the major tegument protein VP8 of bovine herpesvirus-1. Virology 2004;324:327-339.
42 Fornerod M, Ohno M, Yoshida M, Mattaj IW: CRM1 is an export receptor for leucine-rich nuclear export signals. Cell 1997;90:1051-1060.
43 Herold A, Suyama M, Rodrigues JP, Braun IC, Kutay U, Carmo-Fonseca M, Bork P, Izaurralde E: TAP (NXF1) belongs to a multigene family of putative RNA export factors with a conserved modular architecture. Mol Cell Biol 2000;20:8996-9008.
44 Kang Y, Cullen BR: The human Tap protein is a nuclear mRNA export factor that contains novel RNA-binding and nucleocytoplasmic transport sequences. Genes Dev 1999;13:1126-1139.
45 Nigg EA: Nucleocytoplasmic transport: signals, mechanisms and regulation. Nature 1997;386:779-787.
46 Goldfarb DS, Corbett AH, Mason DA, Harreman MT, Adam SA: Importin alpha: a multipurpose nuclear-transport receptor. Trends Cell Biol 2004;14:505-514.
47 Palacios I, Weis K, Klebe C, Mattaj IW, Dingwall C: RAN/TC4 mutants identify a common requirement for snRNP and protein import into the nucleus. J Cell Biol 1996;133:485-494.
48 Ushijima R, Sakaguchi N, Kano A, Maruyama A, Miyamoto Y, Sekimoto T, Yoneda Y, Ogino K, Tachibana T: Extracellular signal-dependent nuclear import of STAT3 is mediated by various importin alphas. Biochem Biophys Res Commun 2005;330:880-886.
49 Harel A, Forbes DJ: Importin beta: conducting a much larger cellular symphony. Mol Cell 2004;16:319-330.
50 Chi NC, Adam EJ, Adam SA: Different binding domains for Ran-GTP and Ran-GDP/RanBP1 on nuclear import factor p97. J Biol Chem 1997;272:6818-6822.
51 Ding Q, Guo H, Lin F, Pan W, Ye B, Zheng AC: Characterization of the nuclear import and export mechanisms of bovine herpesvirus-1 infected cell protein 27. Virus Res 2010;149:95-103.
52 Cansizoglu AE, Lee BJ, Zhang ZC, Fontoura BM, Chook YM: Structure-based design of a pathway-specific nuclear import inhibitor. Nat Struct Mol Biol 2007;14:452-454.
53 Kosugi S, Hasebe M, Entani T, Takayama S, Tomita M, Yanagawa H: Design of peptide inhibitors for the importin alpha/beta nuclear import pathway by activity-based profiling. Chem Biol 2008;15:940-949.
54 Fang CY, Lee CH, Wu CC, Chang YT, Yu SL, Chou SP, Huang PT, Chen CL, Hou JW, Chang Y, Tsai CH, Takada K, Chen JY: Recurrent chemical reactivations of EBV promotes genome instability and enhances tumor progression of nasopharyngeal carcinoma cells. International Journal of Cancer 2009;124:2016-2025.
55 Funk C, Ott M, Raschbichler V, Nagel CH, Binz A, Sodeik B, Bauerfeind R, Bailer SM: The Herpes Simplex Virus Protein pUL31 Escorts Nucleocapsids to Sites of Nuclear Egress, a Process Coordinated by Its N-Terminal Domain. PLoS Pathog 2015;11:e1004957.
56 Goodwin DJ, Hall KT, Stevenson AJ, Markham AF, Whitehouse A: The open reading frame 57 gene product of herpesvirus saimiri shuttles between the nucleus and cytoplasm and is involved in viral RNA nuclear export. J Virol 1999;73:10519-10524.
57 Williams BJ, Boyne JR, Goodwin DJ, Roaden L, Hautbergue GM, Wilson SA, Whitehouse A: The prototype gamma-2 herpesvirus nucleocytoplasmic shuttling protein, ORF 57, transports viral RNA through the cellular mRNA export pathway. Biochem J 2005;387:295-308.
58 Tunnicliffe RB, Hautbergue GM, Kalra P, Jackson BR, Whitehouse A, Wilson SA, Golovanov AP: Structural basis for the recognition of cellular mRNA export factor REF by herpes viral proteins HSV-1 ICP27 and HVS ORF57. PLoS Pathog 2011;7:e1001244.
59 Mattaj IW, Englmeier L: Nucleocytoplasmic transport: the soluble phase. Annu Rev Biochem 1998;67:265-306.
60 Nakielny S, Dreyfuss G: Nuclear export of proteins and RNAs. Curr Opin Cell Biol 1997;9:420-429.